Estimates of modern arc-parallel strain rates in fore arcs

Robert McCaffrey Department of Earth and Environmental Sciences, Rensselaer Polytechnic Institute, Troy, New York 12180

ABSTRACT

Deflections of slip vectors of interplate thrust earthquakes from expected directions are used to estimate arc-parallel strain rates within the overriding plates at the world's major convergent plate margins. Arc-parallel extension strain rates, between 10^{-8}/yr and 10^{-7}/yr and significant at 2 standard deviations, are observed in the fore arcs of the Aegean, Aleutian, Mariana, Sumatran, southern Kuriles, New Hebrides, Scotia, and southern Central American (lat 8° to 12°N) subduction zones and the Himalayas. Northern Chile (lat 17° to 31°S) and Central America (lat 11° to 18°N) show arc-parallel compression. Available geologic and geodetic estimates of fore-arc slip and strain rates agree within a factor of two with slip-vector estimates. Arc-parallel strain in fore arcs is rapid enough to produce geologically significant effects, such as unroofing of high-grade metamorphic rocks and disruption of transported fore-arc terranes. Fore arcs deform even where convergence is perpendicular to curved margins, demonstrating that head-on subduction can produce a three-dimensional strain field.

INTRODUCTION

Along-arc gradients in plate-convergence obliquity produce arc-parallel gradients in the horizontal shear stress on plate-boundary faults, that in turn results in arc-parallel stretching or compression of the fore arc. Using an analog of disks (fore arc) sitting on cardboard (subducting plate) pushed beneath a table top (overriding plate), Avé Lallemant and Guth (1990) showed that the disks will translate and separate as the cardboard is pushed beneath a curved edge of the table. In this analogy, the fore arc moves relative to the landward plate and deforms internally so that both its slip and strain rates are nonzero. However, following this analogy, if the disks are glued to each other and to the table, or the cardboard is greased to reduce friction, the fore arc can behave rigidly, remaining attached to the upper plate, in which case its arc-parallel slip and strain rates are zero. If the disks are glued to each other but not to the table, the fore arc can remain rigid but can translate along a strike-slip fault on the arc side, in which case its strain rate can be zero but its slip rate, relative to the rest of the upper plate (here called the "landward" plate), is not. Thus, the response of a particular fore arc will depend both on the strength of the "glue" holding it together and the shear stress acting on it. In this paper I use deflections of earthquake slip vectors from expected relative plate-convergence directions to estimate arc-parallel slip rates of fore arcs relative to their landward plate and to estimate arc-parallel strain rates from changes in slip rates along strike.

DATA AND METHODS

Consider the subducting plate, the fore arc, and the landward plate of a subduction zone as a three-plate system. The fore arc and the landward plate are both part of the overriding plate but may be in relative motion. The landward and subducting plates are assumed to be rigid, and their relative motion is described by a pole of rotation. The direction of motion of the subducting plate relative to the fore arc is estimated from slip vectors of interplate earthquakes. Because the instantaneous velocity vectors for the three plates cancel at any point in space, the local rate of motion of the fore arc relative to the landward plate in the direction parallel to the arc is $v_s = v(\sin\gamma - \cos\gamma \tan\psi)$, where v is the plate-convergence rate, γ is the plate-convergence obliquity (trench-normal azimuth minus the relative plate-vector azimuth), and ψ is the slip-vector obliquity (trench-normal azimuth minus the slip-vector azimuth) (McCaffrey, 1994). This rate strictly holds only at the earthquake hypocenter, which is on the plate interface. The arc-parallel strain rate is the gradient of v_s in the direction parallel to the arc.

Criteria used to select the interplate earthquakes from which slip vectors are taken are as follows: they are shallower than 60 km depth, they occur between the trench and the volcanic arc, they have a nodal plane that dips at less than 45° and toward the arc (i.e., the dip direction is rotated arcward from the trench), and they have a thrust component. At fore arcs where poles of rotation are not known well, I calculate poles that fit the slip vectors. At several fore arcs, poles can be found that do not require deformation; these are noted in Table 1, although results using published poles are listed. Details of the data analysis are provided in McCaffrey (1994) and results of some southwestern Pacific subduction zones have been modified from McCaffrey (1995) by addition of new data. Slip vectors, trench normals, and plate-motion vectors are averaged in 150-km-long segments of the fore arcs, and v_s is calculated in each of these segments. The strain rate is the slope of a weighted, straight-line fit to v_s as a function of distance along the arc (Fig. 1, Table 1) and is calculated for sections of trenches in which v_s values display a linear trend over several hundred kilometres or more. Sometimes these sections overlap when it is unclear where the boundary should be (Fig. 1). Table 2[1] provides pertinent data and data references.

COMPARISONS TO GEOLOGIC AND GEODETIC RATES

Velocities of Kodiak (at km 590) and Sand Point (at km 1160) in the Alaska fore arc (Fig. 1B) relative to North America from very long baseline interferometry data have arc-parallel components of 3 ± 1 and 5 ± 1 mm/yr (Ma et al., 1990); slip-vector estimates are −10 ± 10 and 3 ± 10 mm/yr, respectively. Three estimates of slip rate on the Sumatra fault (Sieh et al., 1994) and a spreading rate in the Andaman Sea (Curray, 1989) reveal a strain rate (1.7×10^{-8}/yr) identical to the slip-vector estimate, but are on average about 10 mm/yr slower (Fig. 1G). Geodetic measurements (Smith et al., 1994b) show that Australia is moving 10 to 20 mm/yr slower relative to Eurasia than the NUVEL-1A (DeMets et al., 1994) predicts, so the discrepancy may be due to overestimation of the plate-convergence rate.

Global Positioning System (GPS) measurements show that the Nazca plate converges with the South American fore arc near the equator at a larger azimuth than predicted by NUVEL-1A (Freymueller et al., 1993), indicating a 16 ± 6 mm/yr northward motion of the fore arc relative to South America (Fig. 1H); earthquake slip-vector azimuths predict 7 ± 8 mm/yr in the same sense. Duquesnoy et al. (1994) measured 26 ± 5 mm/yr slip on the Philippine fault near 11°N from combined GPS and trilateration (Fig. 1K). Slip vectors at the Philippine

[1]Data Repository item 9602, Data for Fore Arc Bins, is available on request from Documents Secretary, GSA, P.O. Box 9140, Boulder, CO 80301. E-mail: editing@geosociety.org.

Data Repository item 9602 contains additional material related to this article.

TABLE 1. ARC-PARALLEL SLIP AND STRAIN RATES FOR FORE ARCS

Convergent margin segment	Type of deformation*	Range of region (°)	Pole of rotation†	No. Bins/ no. slip vectors	Arc-parallel slip rate (mm/yr)	Arc-parallel strain rate (10^{-8}/yr)	RMS misfit (mm/yr
Aegean	D	19E to 28E	1	6 / 15	2 ± 13	3.2 ± 1.0	8
Alaska	R	195E to 215E	N PA-NA	10 / 104	-1 ± 11	1.3 ± 1.5	16
E. Aleutian	D	173E to 188E	N PA-NA	8 / 212	27 ± 12	2.7 ± 1.0	9
Aleutian	D	164E to 195E	N PA-NA	16 / 322	29 ± 20	3.0 ± 0.8	19
Antilles	R‡	15N to 20N	N SA-CR	5 / 18	-5 ± 2	0.8 ± 0.7	2
Himalaya	D§	74E to 96E	2	8 / 19	2 ± 4	0.7 ± 0.3	7
Izu	T‡	23N to 34N	S PA-PS	8 / 73	-14 ± 6	-1.1 ± 0.6	8
Mariana	D§	11N to 23N	S PA-PS	11 / 63	-15 ± 11	1.9 ± 0.4	7
North Kuriles	R	48N to 55N	N PA-NA	6 / 124	1 ± 1	0.0 ± 0.1	1
South Kuriles	D	41N to 48N	N PA-NA	8 / 248	5 ± 8	1.9 ± 0.2	2
Japan	R	35N to 41N	N PA-NA	5 / 196	-3 ± 3	0.8 ± 0.8	3
Timor-Java	T‡	104E to 126E	N AU-EU	14 / 40	-17 ± 10	0.0 ± 0.4	11
Sumatra	D§	14N to 104E	3	15 / 104	23 ± 15	1.7 ± 0.4	11
South Chile	R	55S to 47S	N AN-SA	3 / 3	-4 ± 5	-0.9 ± 1.5	6
Chile	R	39S to 31S	N NZ-SA	5 / 87	5 ± 4	-0.8 ± 0.5	3
North Chile	D	31S to 17S	N NZ-SA	10 / 88	1 ± 13	-2.9 ± 0.4	4
Peru	R	20S to 3N	N NZ-SA	19 / 69	1 ± 17	0.7 ± 0.5	19
S. Centr. Amer.	D	8N to 13N	N CO-CR	5 / 95	7 ± 8	3.4 ± 0.4	2
N. Centr. Amer.	D‡	11N to 18N	4	12 / 213	-3 ± 9	-1.6 ± 0.2	4
Mexico	T	15N to 19N	N CO-NA	7 / 112	-9 ± 3	-0.5 ± 0.5	3
New Hebrides	D§	173E to 18S	N PA-AU	6 / 103	-49 ± 34	12.0 ± 3.2	17
Philippine	T‡	3N to 14N	S PS-EU	8 / 140	-50 ± 14	1.9 ± 1.5	16
Ryukyu	R‡	23N to 34N	S PS-EU	12 / 45	8 ± 29	1.1 ± 3.7	65
Scotia	D	61S to 55S	P SA-SN	6 / 89	-14 ± 23	13.0 ± 6.1	21
Tonga	D§	23S to 14S	N PA-AU	8 / 241	17 ± 15	3.6 ± 2.4	17
Kermadec	T‡	39S to 23S	N PA-AU	12 / 331	10 ± 4	-0.3 ± 0.3	4
New Zealand	D§	43S to 36S	N PA-AU	6 / 13	19 ± 13	3.2 ± 1.7	11

* R—rigid; T—translating; D—deforming.

† N—DeMets et al. (1994) NUVEL-1A; S—Seno et al. (1993); P—Pelayo and Wiens (1989); AN—Antarctic; AU—Australia; CR—Caribbean; CO—Cocos; EU—Eurasia; NA—North America; NZ—Nazca; PA—Pacific; PS—Philippine Sea plate; SA—South America; SN—Sandwich. 1: Aegean fore arc - Africa pole (41.0°S, 158.6°E, 0.6°/Ma) is sum of fore arc - Eurasia pole from satellite laser ranging vectors at Xrisokelaria, Roumeli, and Katavia (Smith et al., 1994a) and NUVEL-1A Africa - Eurasia pole. 2: India-Eurasia slowed by 1/3 to match estimated convergence rate of 15 mm/yr at Himalayas (Molnar, 1984). 3: India-Australia for Sumatra, India-Eurasia for Andaman. 4: CO-CR for Central America, CO-NA for Mexico. Positive slip rates are right lateral. Positive strain rates are arc-parallel extension. Uncertainties are 1 standard deviation.

‡ A pole of rotation can be found that fits the slip vectors; fore-arc deformation not required.

§ No pole of rotation can be found to fit slip vectors.

trench predict a rate that is a factor of two higher, using the Seno et al. (1993) Philippine Sea–Eurasia pole. Other faults may take up part of the motion because the geodetic network was less than 6 km wide. However, a pole of rotation can be found that matches the slip vectors well enough at the Philippine trench (Fig. 1K) that slip partitioning is not required. Geodetic measurements in North Island, New Zealand, reveal about 30 mm/yr of arc-parallel motion of the fore arc (Walcott, 1984), in agreement with local slip vectors (Fig. 1N).

Two measurements of arc-parallel strain rates in fore arcs compare well. From GPS, Gilbert et al. (1994) estimated an arc-parallel strain rate for the western Aegean of 3 to 8×10^{-8}/yr; slip vectors give a rate of $3.6 \pm 1.0 \times 10^{-8}$/yr (Fig. 1A). Geist et al. (1988) estimated arc-parallel strain in the eastern Aleutian fore arc of 9% to 10% over 5 to 6 m.y. (Fig. 1B), for a strain rate of 1.5 to 2.0 $\times 10^{-8}$/yr; the slip vector estimate is $2.7 \pm 1.0 \times 10^{-8}$/yr.

DISCUSSION

Fore arcs reveal a wide range of kinematic responses to changes in obliquity, from rigidity to complete partitioning of the slip. The fore arcs are classified into rigid (R), translating (T), and deforming (D), as discussed above, on the bases of the slip and strain rates and their uncertainties, and examination of Figure 1 (Table 1). Half of the fore-arc segments have significant strain rates (type D). Of the five translating fore arcs, four do not have poles of rotation known independently of the slip vectors and appear to be rigid when new poles of rotation are calculated. For other fore arcs where poles of rotation are not well known, slip vectors cannot fit a single pole of rotation and fore-arc deformation is required (Fig. 1, Table 1). Arc-parallel slip rates are as high as 50 mm/yr and strain rates reach several parts in 10^{-8}/yr. The Himalaya and Marianas, in particular, have fore arcs that move along the arc at the same rate as the subducting plate. Most strain rates are arc-parallel extensional (positive slope). Only the north Chile and north Central America fore arcs have arc-parallel compression strain rates that are more than two standard deviations away from zero.

Differences between the surface (geologic and geodetic) slip-rate estimates and those from slip vectors, from the base of the fore arc, may be caused either by uncertainties or by vertical gradients in fore-arc slip rates. Vertical gradients are predicted for a viscous fore arc but not for critically tapered perfect plastic and noncohesive Coulomb rheologies (Platt, 1993). Unfortunately, the form of the vertical gradient for the viscous wedge is not known well enough to say whether the observed difference in slip rates between the top and bottom is diagnostic of rheology.

Large volumes of high-pressure–low-temperature metamorphic rocks are often exposed in modern and past fore-arc settings, yet the uplift mechanism is not clear. Uplift occurred when thermal gradients were low enough to prevent retrograde metamorphism, suggesting a steady-state subduction setting. Platt (1986) proposed that sediments accreted to the base of the wedge cause crustal thickening and extension on normal faults striking parallel to the trench. Avé Lallemant and Guth (1990) suggested that arc-parallel stretching of fore arcs due to oblique subduction can result in rapid uplift. During a long history of subduction, blueschists from west-central Baja California apparently rose at 0.1 mm/yr along shallow-dipping normal faults that strike nearly perpendicular to the old trench (Baldwin and Harrison, 1989; S. Baldwin, 1995, personal commun.).

Arc-parallel strain rates observed in modern fore arcs are high enough to allow geologically rapid uplift of deep fore-arc rocks. Assuming that the fore arc is incompressible, $\dot{\varepsilon}_{xx} + \dot{\varepsilon}_{yy} + \dot{\varepsilon}_{zz} = 0$, where x is perpendicular to the fore arc, y is parallel to it, z is down, and $\dot{\varepsilon}_{xx}$ represents the normal strain rate in the x direction, for example. Slip vectors suggest that $\dot{\varepsilon}_{yy}$ is commonly positive (extensional), and it is likely that $\dot{\varepsilon}_{xx}$ and $\dot{\varepsilon}_{zz}$ are either negative (compressive) or zero. Bounding cases are $\dot{\varepsilon}_{zz} \approx 0$ (arc-normal shortening by strike-slip faulting) and $\dot{\varepsilon}_{xx} \approx 0$ (crustal thinning by normal faulting). Strike-slip faults at high angles to the trench can transport deep rocks seaward and upward along the dipping thrust fault (Karig, 1980). In this case, $\dot{\varepsilon}_{xx} = -\dot{\varepsilon}_{yy}$, and the rate at which rocks approach the surface of the

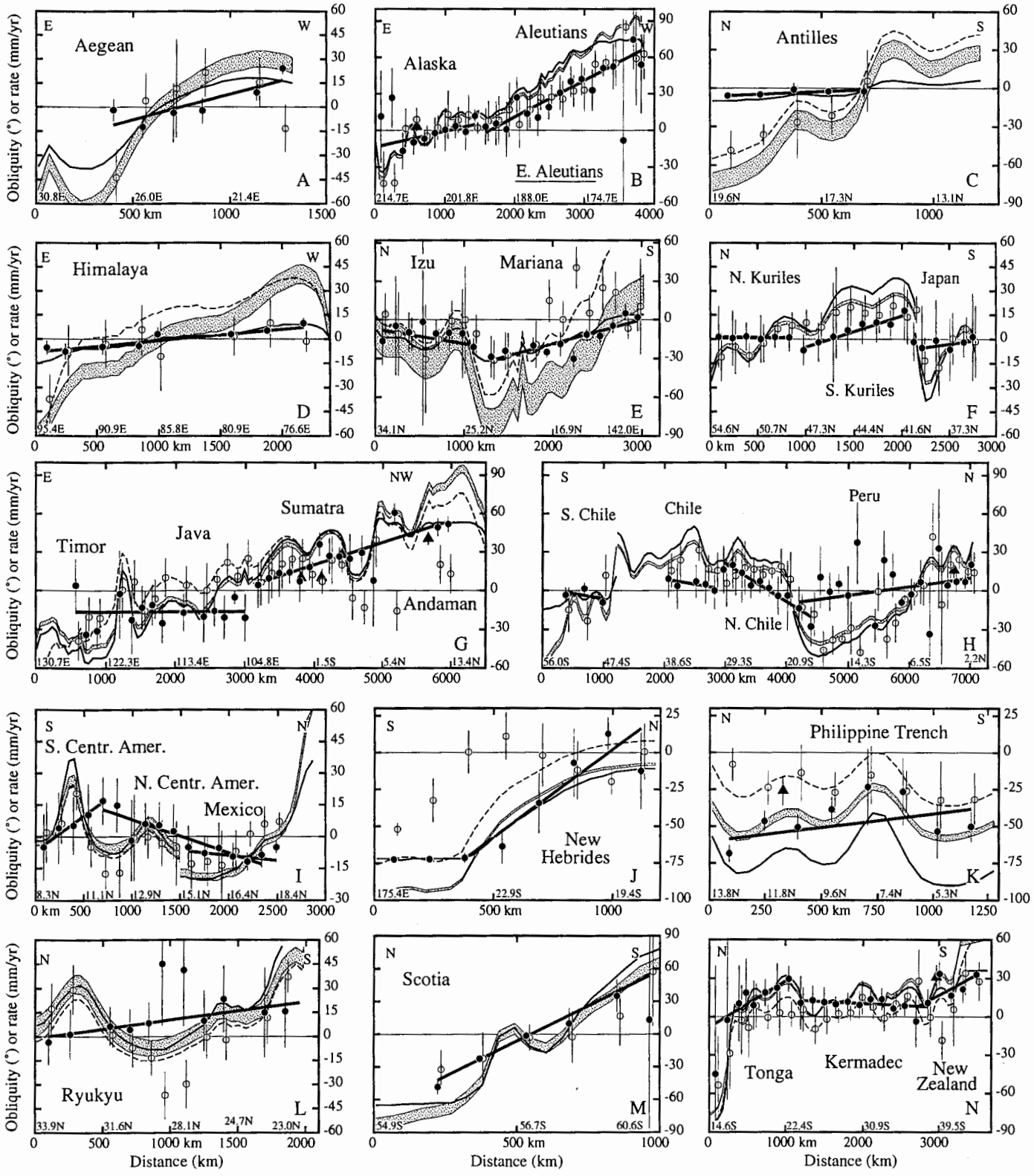

Figure 1. Plot of plate-convergence obliquity (γ, shaded curves), slip-vector obliquity (ψ, open circles), arc-parallel fore-arc slip rates (v_s, solid circles), and arc-parallel slip rate of subducting plate (thin solid curve) along subduction zones. Thin dashed curves, when present, show plate obliquity from poles of rotation based on best fit to slip vectors at trench. Horizontal axis is distance in kilometres along deformation front or trench (also labeled with approximate latitude or longitude). Vertical axis is angles in degrees and mm/yr (labeled at right of each plot). Positive v_s indicates right-lateral shear; negative values are left lateral. Heavy dark straight lines show weighted, best fit to v_s, slope of which is arc-parallel strain rate (Table 1). Positive slopes show arc-parallel extension; negative slopes show arc-parallel compression. Triangles show geodetic and geologic estimates of arc-parallel slip rates from published observations (see text).

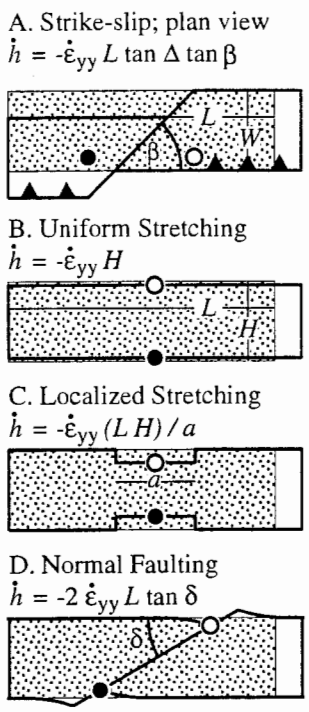

Figure 2. Mechanisms of fore-arc stretching. A is map view and B through D are cross sections. Shaded box shows original shape of fore arc and solid lines show shape after 10% strain (isostasy is ignored). *L* is length parallel to arc (y direction); *W* is width of fore arc (x direction); *H* is depth (z direction); Δ is dip angle of thrust fault; $\dot{h}$ is vertical component of rate at which solid circle (at base of fore arc) approaches open circle (at surface of fore arc).

fore arc is $\dot{h} = -\dot{\varepsilon}_{yy} L \tan \Delta \tan \beta$, where L is the along-strike distance between strike-slip faults, Δ is the subduction-zone dip angle, and β is the angle that the strike-slip fault makes with the trench axis (Fig. 2A). Using $\Delta = 10°$, $\beta = 45°$, $L = 100$ km, and a strain rate of 10^{-8}/yr, $\dot{h} = 0.2$ mm/yr. However, with time, the fault-bounded fore-arc blocks will rotate, resulting in decrease in both β and the rate of uplift.

For uniform stretching of the fore arc in the y-z plane (vertical plane parallel to arc), $\dot{\varepsilon}_{zz} = -\dot{\varepsilon}_{yy}$, and the rate of crustal thinning is $\dot{h} = -\dot{\varepsilon}_{yy} H$ (Fig. 2B). Thus, a rock at 30 km depth approaches the surface at 0.3 mm/yr for a strain rate of 10^{-8}/yr. Localized stretching within a zone of width a (Fig. 2C) amplifies $\dot{h}$, relative to uniform stretching, by a factor L/a, and arc-perpendicular normal faults dipping at angle δ (Fig. 2D) do so by 2 (L/H) tan δ, when the faults or high strain areas occur at an average along-strike spacing of L. For example, using $L = 100$ km, $a = 30$ km, $H = 30$ km, and $\delta = 30°$, localized strain and normal faulting both magnify $\dot{h}$ by about a factor of 3. Many fore arcs show extensional strain rates in excess of 2×10^{-8}/yr, suggesting that by these mechanisms deep rocks may approach the surface at rates approaching 1 mm/yr. Isostasy will slow the ascent of the deeper rocks relative to sea level, but if the fore arc is thickened by underplating subducted sediments so as to maintain fairly constant crustal thickness, the deep rocks will rise relative to sea level at the rate $\dot{h}$.

The high strain rates observed in modern fore arcs have implications for other aspects of subduction-zone dynamics. First, there is little evidence for wholesale arc-parallel translation of rigid fore arcs (Jarrard, 1986; Beck, 1991). With the exception of Java and the Izu arcs, where plate motions are poorly constrained, all fore arcs that translate faster than 1 cm/yr have strain rates of 2×10^{-8}/yr or more. Thus, fore arcs are probably not transported far without observable internal disruption, and any detached fore-arc slivers are not very large. Using Sumatra and the Aleutians as examples, there will be about 70% and 100% strain in the fore arcs when they have been translated an average of 1000 km. The block-faulted structure of the Aleutian fore arc (Geist et al., 1988) is probably typical of translating fore arcs. Second, subduction can be perpendicular to the trench (plate obliquity is near zero), yet arc-parallel strain rates remain large; e.g., at the Aegean, Himalaya, northern Chile, and Scotia fore arcs where there are strong gradients in the obliquity (Fig. 1). Thus, along with strain in the vertical plane of the convergence vector, head-on subduction around a curved margin produces three-dimensional deformation of fore arcs.

SUMMARY AND CONCLUSIONS

Modern arc-parallel strain rates are estimated from deflections of interplate earthquake slip vectors. Extensional strain is more common than compression, at rates of 10^{-8}/yr to 10^{-7}/yr. Strain rates are fast enough to have significant geologic consequences, such as disrupting fore-arc terranes and allowing high-grade metamorphic rocks to approach the surface of the fore arc at rates approaching 1 mm/yr.

ACKNOWLEDGMENTS

Supported by National Science Foundation grant EAR-9105050. H. Avé Lallemant and J. Platt provided helpful reviews.

REFERENCES CITED

Avé Lallemant, H. G., and Guth, L. R., 1990, Role of extensional tectonics in exhumation of eclogites and blueschists in an oblique subduction setting, northwest Venezuela: Geology, v. 18, p. 950–953.

Baldwin, S. L., and Harrison, T. M., 1989, Geochronology of blueschists from west-central Baja California and the timing of uplift in subduction complexes: Journal of Geology, v. 97, p. 149–163.

Beck, M. E., 1991, Coastwise transport reconsidered: Lateral displacements in oblique subduction zones, and tectonic consequences: Physics of the Earth and Planetary Interiors, v. 68, p. 1–8.

Curray, J. R., 1989, The Sunda Arc: A model for oblique plate convergence, *in* van Hinte, J. E., et al., eds., Proceedings, Symposium on Snellius-II Expedition, Jakarta, Volume 1, Geology and geophysics of the Banda arc and adjacent areas: Netherlands Journal of Sea Research, v. 24, p. 131–140.

DeMets, C., Gordon, R. G., Argus, D. F., and Stein, S., 1994, Effects of recent revisions to the geomagnetic reversal time scale on estimates of current plate motions: Geophysical Research Letters, v. 21, p. 2191–2194.

Duquesnoy, T., Barrier, E., Kasser, M., Aurelio, M., Gaulon, R., Punongbayan, R. S., Rangin, C., and the French-Philippine Cooperation Team, 1994, Detection of creep along the Philippine fault: First results of geodetic measurements on Leyte island, central Philippine: Geophysical Research Letters, v. 21, p. 975–978.

Freymueller, J. T., Kellog, J. N., and Vega, V., 1993, Plate motions in the north Andean region: Journal of Geophysical Research, v. 98, p. 21,853–21,863.

Geist, E. L., Childs, J. R., and Scholl, D. W., 1988, The origin of summit basins of the Aleutian Ridge: Implications for block rotation of an arc massif: Tectonics, v. 7, p. 327–341.

Gilbert, L., Kastens, K., Hurst, K., Paradissis, D., Veis, G., Billiris, H., Hoppe, W., and Schluter, W., 1994, Strain results and tectonics from the Aegean GPS experiment: Eos (Transactions, American Geophysical Union), v. 75, p. 116.

Jarrard, R. D., 1986, Terrane motion by strike-slip faulting of fore arc slivers: Geology, v. 14, p. 780–783.

Karig, D. E., 1980, Material transport within accretionary prisms and the "knocker" problem: Journal of Geology, v. 88, p. 27–39.

Ma, C., Sauber, J. M., Bell, L. J., Clark, T. A., Gordon, D., Himwich, W. E., and Ryan, J. W., 1990, Measurement of horizontal motions in Alaska using Very Long Baseline Interferometry: Journal of Geophysical Research, v. 95, p. 21,991–22,011.

McCaffrey, R., 1994, Global variability in subduction thrust zone–fore arc systems: Pure and Applied Geophysics, v. 141, p. 173–224.

McCaffrey, R., 1995, Slip partitioning at convergent plate boundaries of SE Asia: Geological Society of London Journal.

Molnar, P., 1984, Structure and tectonics of the Himalaya: Constraints and implications of geophysical data: Annual Review of Earth and Planetary Sciences, v. 12, p. 489–518.

Pelayo, A. M., and Wiens, D. A., 1989, Seismotectonics and relative plate motions of the Scotia Sea region: Journal of Geophysical Research, v. 94, p. 7293–7320.

Platt, J. P., 1986, Dynamics of orogenic wedges and the uplift of high-pressure metamorphic rocks: Geological Society of America Bulletin, v. 97, p. 1037–1053.

Platt, J. P., 1993, Mechanics of oblique convergence: Journal of Geophysical Research, v. 98, p. 16,239–16,256.

Seno, T., Stein, S., and Gripp, A., 1993, A model for the motion of the Philippine Sea plate consistent with NUVEL-1 and geological data: Journal of Geophysical Research, v. 98, p. 17,941–17,948.

Sieh, K., Zachariasen, J., Bock, Y., Edwards, L., Taylor, F., and Gans, P., 1994, Active tectonics of Sumatra: Geological Society of America Abstracts with Programs v. 26, no. 7, p. A382.

Smith, D. E., Kolenkiewicz, R., Robbins, J. W., Dunn, P. J., and Torrence, M. H., 1994a, Horizontal crustal motion in the central and eastern Mediterranean inferred from satellite laser ranging measurements: Geophysical Research Letters, v. 21, p. 1979–1982.

Smith, D. E., and eight others, 1994b, Contemporary global horizontal crustal motion: Geophysical Journal International, v. 119, p. 511–520.

Walcott, R. I., 1984, The kinematics of the plate boundary zone through New Zealand: A comparison of short- and long-term deformations: Royal Astronomical Society Geophysical Journal, v. 79, p. 613–633.

Manuscript received July 5, 1995
Revised manuscript received September 29, 1995
Manuscript accepted October 12, 1995